

学号
Student No.: 2023280024

西北工业大学研究生学位论文选题报告表
Northwestern Polytechnical University
Graduate Degree Dissertation Title Selection Report Form

学 院	民航学院
School	School of Civil Aviation
学科、专业	航空宇航科学与技术
Discipline / Specialty	Aerospace Science and Technology
姓 名	
Name	DHAKAL AMRIT
学位 级别	硕士
Degree	Master
导 师	吴宇
Supervisor	Wu Yu
培养 类别	留学研究生
Category	Overseas Postgraduates
报告 日期	2024 年 12 月 20 日
Date of Report	December 20 th 2024

研 究 生 院
Graduate School

研究生学位论文选题报告的要求

- 一、硕士生的选题报告内容应包括文献综述、选题意义、研究内容、研究方案，论文工作量的估计、工作条件，预期达到的水平，存在的问题及拟采取的解决措施。
- 二、博士生的选题报告内容应包括文献综述、选题背景及其意义、研究内容、研究特色、工作难点、预期成果及其可能的创新点。
- 三、选题报告会应以学术活动的方式公开进行。
- 四、正式开题之前，研究生应在广泛阅读中、外文资料的基础上，深入了解拟选课题的国内外研究动态，把握所选课题的目的、意义和预期结果，明确课题工作的设想、方法和研究路径。
- 五、研究生在规定的时间内，写出选题报告初稿，经指导教师审阅同意后，由指导教师安排选题报告时间。选题报告未通过者，重新开题，若第二次选题报告仍通不过者，则按有关规定终止学籍。
- 六、选题报告不能按期完成者，应及时向研究生院培养处提出延期申请。
- 七、本表可以打印或用钢笔认真填写，若不够填写时，可另加附页。

Requirements for the Dissertation Title Selection Report

1. The Dissertation Title Selection Report for Master Degrees should include the Literature Review, the Meaning of the Title Selection, the Research Contents, the Research Plan, Workload Estimation, Working Conditions, the Goal to Achieve, Problems Existing as well as the Measures to Take.
2. The Dissertation Title Selection Report for PhD Degrees should include Literature Review, Background and Meaning of the Selection, Research Contents, Characteristics of the Research, Difficulties, Goals to Achieve and possible Innovations.
3. The Report should be made in public as academic activities.
4. Before starting the title, graduates should, based on the extensive reading through the literature both in Chinese and in foreign languages, have a deep command of the research tendency home and abroad,. They must have a clear mind of the aim, meaning and foreseen results, research assumption, methods and approaches.
5. Graduates should finish the draft report within the required time, and then the supervisor after having checked the report, organizes time to make the report. Those who fail to pass the report have to reopen a title. If it can not be passed for a second time, the studentship will be stopped.
6. Those who can not finish the report on time should forward application to the Graduate School to extend the duration.
7. The form should be filled out in pen or printed. If the pages are not enough, extra pages can be attached.

论文题目 Dissertation Title	States estimation of Li ion battery using Equivalent circuit and data driven methods			
论文类型 (在有关项目下作记号√) Dissertation Type (Put a tick √ under relevant item)	基础研究 Fundamental Research	应用研究 Application Research	工程技术 Engineering Technology	跨学科研究 Research Cross Discipline
		√		

研究生在进行选题报告、听取意见后，整理成文（不少于 3500 字）。

1. Research Background

The global energy landscape is under significant pressure due to the limited availability of fossil fuels and their detrimental environmental effects. To align with the goal of limiting global warming to 2°C, a substantial portion of fossil fuel reserves must remain unutilized—approximately one-third of oil, half of natural gas, and over 80% of coal reserves should not be exploited during the period between 2010 and 2050 [1]. These constraints suggest that resource development in the Arctic and the expansion of unconventional oil extraction are incompatible with effective climate change mitigation strategies. Currently, global energy consumption, amounting to roughly 13 terawatts, is predominantly driven by fossil fuels, with oil consumption alone reaching a staggering rate of nearly 1,000 barrels per second [2]. This imminent peak in fossil fuel production, combined with escalating climate concerns, underscores the urgent need to transition to sustainable energy alternatives, presenting critical challenges for future generations. A key technology for lowering reliance on fossil fuels and addressing climate change is lithium-ion batteries, or LIBs. By incorporating LIBs into hybrid power systems, the shipping sector may be able to cut CO₂ emissions by as much as 8.7% [3]. Because they are more affordable and have better performance, lithium-ion batteries (LIBs) are becoming essential for renewable energy storage and electric cars[4].

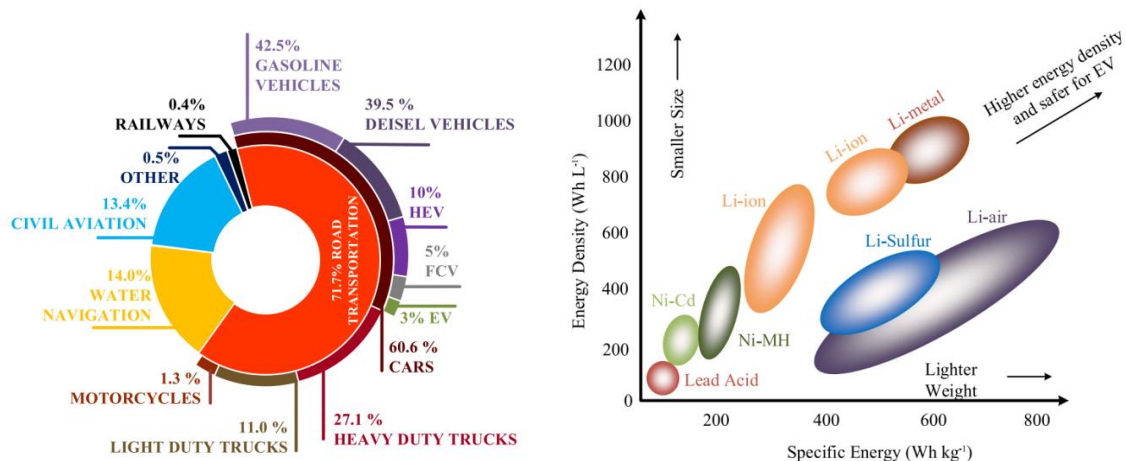



Figure 1. (a) Vehicle CO₂ emission levels and (b) Energy density and specific energy of various batteries at cell level[5]

Recently, there has been a significant surge in the demand for electrical energy, driven by its essential role in various sectors such as industrial manufacturing, homes, entertainment, commercial devices, information technology, and notably, the emerging electric vehicle (EV) industry, spurred by the global

energy crisis and fuel shortages. Given its global importance, it is crucial to ensure the economical use of electrical energy[6]. At smaller scales, such as in wind and solar power generation or electric vehicles, Battery Energy Storage Systems (BESS) are commonly employed. These systems consist of batteries, or battery arrays, that store electrical energy and release it efficiently based on consumption needs. Since Sony introduced lithium-ion batteries to the consumer electronics market in 1990, they have become the dominant choice in various industries due to their superior performance over nickel-metal hydride (NiMH) and traditional lead-acid batteries. The main advantages of lithium-ion batteries include high efficiency, long cycle life, and low self-discharge rates [7]. With extensive research and development in the electric and hybrid vehicle sectors, lithium-ion batteries have emerged as the preferred option due to their ideal characteristics for meeting the demands of the electric vehicle industry [8].

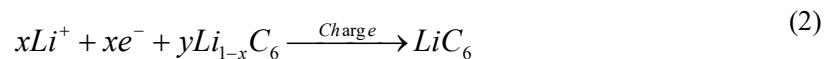
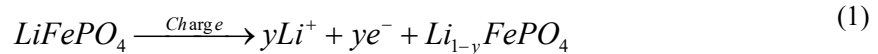
Lithium-ion (Li-ion) batteries are the primary type of batteries used in electrified vehicles today. Additionally, they hold significant potential for stationary energy storage applications. Due to the relatively lightweight and low density of lithium, Li-ion batteries offer higher specific energies compared to batteries made from other materials, such as zinc and lead, as illustrated in **Figure 1(b)**. They come in various shape and sizes as shown in **Figure 2**.



	Cylindrical cell	Prismatic cell	Pouch cell
Design for manufacture	★★ Easy for cell manufacture; Hard for pack manufacture	★★★ Hard for cell manufacture; Easy for pack manufacture	★★★ Easy for cell manufacture, Little hard for pack manufacture
Thermal characteristic	★ Poor heat dissipation since relatively low specific surface area	★★ Specific surface area related to the capacity	★★★ Usually large surface area.
Capacity Density	★★ High.	★★ Depends on cell capacity	★★★ High.
Life	★ Usually less deformation but huge stress and less electrolyte.	★★★ Usually more electrolyte.	★★★ Usually poor electrolyte, uniform deformation.
Safety	★★ Usually little capacity.	★ Usually large capacity and easy to explode.	★★★ Usually no explosion.
Cell to Module Efficiency	★ Low efficiency, hard to design TMS.	★★★ High efficiency, Easy to design TMS.	★★ Low efficiency, easy to design TMS.

Figure 2. Comparison of Different types of cell (a) Cylindrical cell (b) Prismatic cell (c) Pouch cell

Several basic components make up cells. These comprise an electrolyte, a separator, a positive electrode (cathode), and a negative electrode (anode). Current collectors unique from the electrodes themselves may also be found in specific types of cells. A lithium-ion cell is seen schematically in **Figure 4**. The electrochemical storage processes in charge direction for the LiFePO₄-graphite system can be described by the equations 1 and 2 respectively as follows:



Where $0 \leq x \leq 1$, to describe the level of lithiation of a negative electrode and $0 \leq y \leq 1$ of positive electrode[36]

During a typical charge, electrons move from the cathode and transfer to the anode through the external

circuit. In the meantime, Li^+ ions de-intercalate from the cathode and travel through the electrolyte to the anode. During the discharge, the whole process is reversed. There have been three important processes during the intercalation of Lithium ions into the negative electrode: First, Li^+ ions are separated from the positive electrode, and then Li^+ ions diffuse through the electrolyte to the negative electrode, and finally, they are intercalated into the inner layer of negative electrode by passing the solid electrolyte interface (SEI), and it is common that last step is known as charge-transfer process[9].

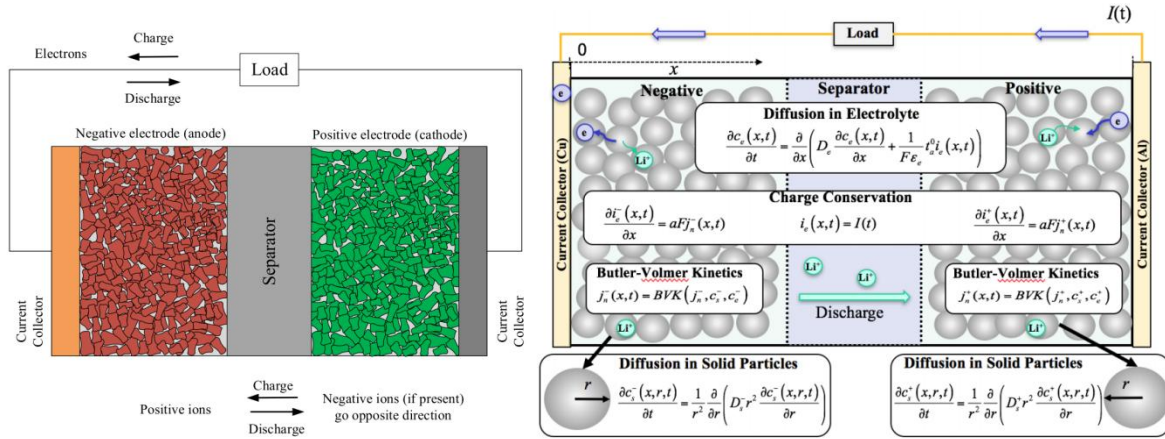


Figure 3. Schematic and structure Diagram of Li ion Cell and the governing equations of the physics process in each part of the battery[9][10]

Table 1 Li-ion battery types

Battery Types	Cathode Materials	Anode Materials	Nominal Voltage (V)	Life Cycle	Energy Density (Wh.L ⁻¹)	Cost	Safety
Lithium Iron Phosphate (LiFePO ₄)	LiFePO ₄	Graphite	3.2	high	Low	high	Safest Li-ion cell chemistry
Lithium Cobalt Oxide (LiCoCO ₂)	LiCoCO ₂	Graphite	3.6	medium	high	low	Highest safety concern
Lithium Manganese Cobalt oxide (LiNiMnCoCO ₂)	LiNiMnC oCO ₂	Graphite	3.6	medium	high	medium	Good safety
Lithium Manganese oxide	LiMnO ₂	Graphite	3.7	low	low	medium	Good safety
Lithium Nickel Cobalt Aluminum oxide (LiNiCoAlO ₂)	LiNiCoAl O ₂	Graphite	3.6	medium	high	medium	Safety concern required

2. Research status of modeling methods and state estimation for lithium-ion battery systems

Models can be helpful tools for designing electrodes, cells, and packs by forecasting a battery's key performance parameters, such as capacity and lifetime. Researchers can use models to investigate the design space for several factors to be used in determining key design elements of batteries such as electrode structure or thermal management. Moreover, mathematical modeling of Li-Ion batteries can be useful for developing battery management systems (BMSs) for both electric vehicles and grid-connected battery systems. The battery and its management system are the most important components of EVs[11]

It can be used as a way to determine the operating limits for certain applications that produce the best lifespan.

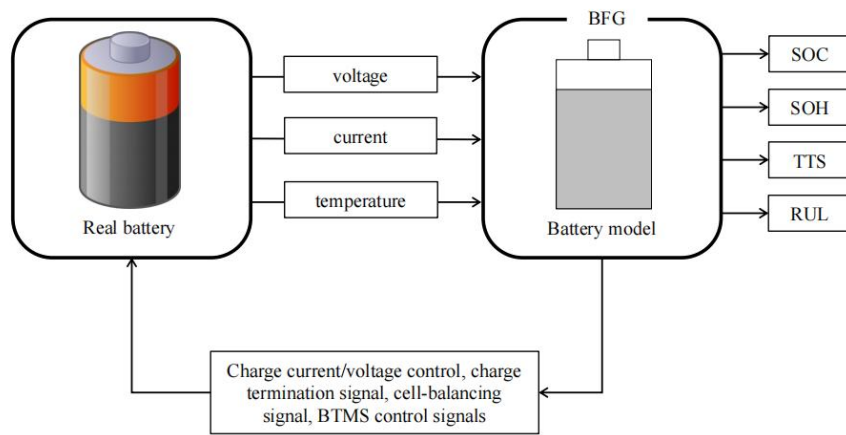


Figure 4. Role of battery modelling in Battery Management System

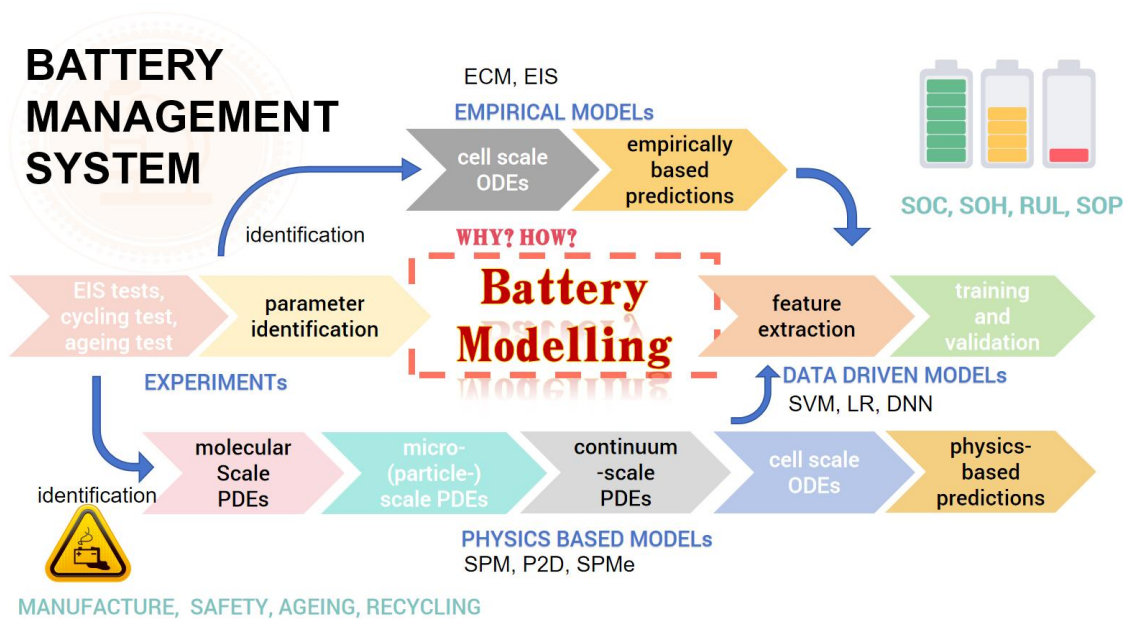


Figure 5. Lithium-Ion battery Modelling[5]

The following will describe the three main categories of lithium battery models.

2.1. Physics-based Model (Electrochemical Model)

The research team of John Newman, M. Doyle and colleague at the University of California, Berkeley were the first to propose and systematically establish an electrochemical mechanism model considers mass transfer, diffusion, migration, and reaction kinetics for lithium-ion batteries [12][13][14][15][16]. The lithium-ion battery models in these literature are one-dimensional models along the thickness direction of the battery as shown in the **Figure 3**. The model is based on Fick's law and concentration solution theory to establish a system of partial differential equations to solve the diffusion of lithium ions in the electrode and the diffusion and migration of lithium ions in the electrolyte. The electrochemical reaction kinetics and thermodynamic equations, such as Butler Volmer, are used to solve the insertion and extraction of lithium ions in porous electrodes, providing a comprehensive description of the mechanism and process of lithium-ion batteries. Due to the limitations of one-dimensional models in describing and calculating the current and temperature distribution at different positions of the battery, as well as the inability to incorporate battery terminals into the model, many scholars have improved their models based on the research of John Newman's team according to different needs, extending the mechanism model to pseudo two dimensional, two-dimensional, pseudo three dimensional, or three-dimensional models. Doyle and Newman proposed a pseudo two dimensional model based on their own model, which describes the electrochemical reactions inside the battery by describing the electrolyte between the porous electrode composed of multiple spherical particles and single particle. We can see these partial differential equations, boundary conditions and initial values below in more detail[17].

2.1.1. EQUATION I: Charge conservation in solid

PDE:
$$\frac{\partial}{\partial x} \sigma_{\text{eff}}^r \frac{\partial}{\partial x} \phi_s^r = a_s^r F j^r, \quad (3)$$

Boundary conditions :
$$\sigma_{\text{eff}}^n \frac{\partial}{\partial x} \phi_s^n \Big|_{x=0} = \sigma_{\text{eff}}^p \frac{\partial}{\partial x} \phi_s^p \Big|_{x=L^{\text{tot}}} = \frac{-i_{\text{app}}}{A}, \quad (4)$$

$$\frac{\partial}{\partial x} \phi_s^n \Big|_{x=L^n} = \frac{\partial}{\partial x} \phi_s^p \Big|_{x=L^n+L^s} = 0, \quad (5)$$

Initial values:
$$\phi_{s,0}^n = 0, \phi_{s,0}^p = u_{\text{ocp}}^p(\theta_{s,0}^p) - u_{\text{ocp}}^n(\theta_{s,0}^n), \quad (6)$$

Where,

σ_{eff}^r is the effective conductivity of the electrode,

ϕ_s^p is the potential in the solid electrode

a_s^r is the specific interfacial surface area of the electrode

F is Faraday's constant

j^r is the lithium flux(rate of lithium movement between solid electrode particle and the electrolyte)

$-i_{\text{app}}$ is the electrical current measured at the terminals of the cell

$L^{\text{tot}} = L^n + L^s + L^p$, is the thickness of the negative electrode, separator and positive electrode

A is the surface area

$\theta_s^r = c_s^r / c_{s,\text{max}}^r$ is the stoichiometry of the electrode such that

$0 \leq \theta_s^r \leq 1$, $\theta_{s,0}^r = c_{s,0}^r / c_{s,\text{max}}^r$ is the initial equilibrium stoichiometry of the electrode

$u_{\text{ocp}}^p(\theta_s^r)$ is the open circuit potential(OCP) of the electrode as a function of local stoichiometry

This equation applies only to the negative and positive electrode of the cell. It is a linear diffusion equation describing electron movement, with a forcing term that models flux of electrons

2.1.2. EQUATION II: Mass conservation in solid

PDE:
$$\frac{\partial c_s^r}{\partial t} = \frac{1}{r^2} \frac{\partial}{\partial r} \left(D_s^r r^2 \frac{\partial c_s^r}{\partial r} \right), \quad (7)$$

Boundary conditions :
$$D_s^r \frac{\partial c_s^r}{\partial r} \Big|_{r=R_s^r} = j^r, \quad (8)$$

$$D_s^r \frac{\partial c_s^r}{\partial r} \Big|_{r=0} = 0. \quad (9)$$

Initial values:
$$c_{s,0}^r = c_{s,max}^r (\theta_0^r + z_0(\theta_{100}^r - \theta_0^r)), \quad (10)$$

Where,

D_s^r is the solid diffusivity of the electrode

$0 \leq z_0 \leq 1$ is the initial cell SOC,

θ_0^r is the value of θ_s^r when the cell is resting at 0% SOC,

θ_{100}^r is the value of θ_s^r when the cell is resting at 100% SOC

This equation is also valid for negative and positive electrode of the region. Lithium motion inside electrode particle is modeled as standard linear diffusion.

2.1.3. EQUATION III: Charge conservation in electrolyte

PDE:
$$\frac{\partial}{\partial x} \kappa_{eff}^r \left(\frac{\partial}{\partial x} \phi_e^r + \frac{2RT(t_+^0 - 1)}{F} \left(1 + \frac{\partial \ln f_{\pm}}{\partial \ln c_e} \right) \frac{\partial \ln c_e^r}{\partial x} \right) + a_s^r F j^r = 0, \quad (11)$$

Boundary conditions :
$$-\kappa_{eff}^r \left[\frac{\partial}{\partial x} \phi_e^r + \frac{2RT(t_+^0 - 1)}{F} \left(1 + \frac{\partial \ln f_{\pm}}{\partial \ln c_e} \right) \frac{\partial \ln c_e^r}{\partial x} \right] \Big|_{x=0}^{x=L^{tot}} = 0, \quad (12)$$

$$-\kappa_{eff}^r \left[\frac{\partial}{\partial x} \phi_e^r + \frac{2RT(t_+^0 - 1)}{F} \left(1 + \frac{\partial \ln f_{\pm}}{\partial \ln c_e} \right) \frac{\partial \ln c_e^r}{\partial x} \right] \Big|_{x=L^n}^{x=L^n+L^s} = \frac{i_{app}}{A}, \quad (13)$$

Initial values:
$$\phi_{e,0}^r = -u_{ocp}^n(\theta_{s,0}^n). \quad (14)$$

Where

κ_{eff}^r is the effective conductivity of the electrolyte

R is the Universal gas constant

t_+^0 is the transference number of the positive ion in the electrolyte with respect to the solvent and

f_{\pm} is the mean molar activity coefficient

2.1.4. EQUATION IV: Mass conservation in electrolyte

PDE:
$$\frac{\partial \epsilon_e^r c_e^r}{\partial t} = \frac{\partial}{\partial x} D_{e,eff}^r \frac{\partial}{\partial x} c_e^r + a_s^r (1 - t_+^0) j^r, \quad (15)$$

$$\text{Boundary conditions : } \frac{\partial c_e^n}{\partial x} \Big|_{x=0} = \frac{\partial c_e^p}{\partial x} \Big|_{x=L^{\text{tot}}} = 0 , \quad (16)$$

$$D_{e,\text{eff}}^n \frac{\partial c_e^n}{\partial x} \Big|_{x=(L^n)^-} = D_{e,\text{eff}}^s \frac{\partial c_e^s}{\partial x} \Big|_{x=(L^n)^+} , \quad (17)$$

$$D_{e,\text{eff}}^s \frac{\partial c_e^s}{\partial x} \Big|_{x=(L^n+L^s)^-} = D_{e,\text{eff}}^p \frac{\partial c_e^p}{\partial x} \Big|_{x=(L^n+L^s)^+} , \quad (18)$$

$$c_e^n \Big|_{x=(L^n)^-} = c_e^s \Big|_{x=(L^n)^+} , \quad (19)$$

$$c_e^s \Big|_{x=(L^n+L^s)^-} = c_e^p \Big|_{x=(L^n+L^s)^+} , \quad (20)$$

$$\text{Initial values: } c_e = c_{e,0} \quad (21)$$

Where

ϵ_e^r is the porosity (volume fraction of the electrolyte in the cell region)

$D_{e,\text{eff}}^r$ is the diffusivity of lithium ion in the electrolyte

2.1.5. EQUATION V: Kinetics(Butler-Volmer Equation)

$$\text{PDE: } j^r = j_0^r \left\{ \exp \left(\frac{(1-\alpha^r)F}{RT} \eta^r \right) - \exp \left(\frac{\alpha^r F}{RT} \eta^r \right) \right\} , \quad (22)$$

$$j_0^r = k_{\text{norm},0}^r \left(\frac{c_e^r}{c_{e,0}^r} \right)^{1-\alpha^r} \left(1 - \frac{c_{s,e}^r}{c_{s,\text{max}}^r} \right)^{1-\alpha^r} \left(\frac{c_{s,e}^r}{c_{s,\text{max}}^r} \right)^{\alpha^r} , \quad (23)$$

$$\eta^r = \phi_s^r - \phi_e^r - u_{\text{ocp}}^r \left(\frac{c_{s,e}^r}{c_{s,\text{max}}^r} \right) - FR_f^r j^r , \quad (24)$$

Where

α^r is the charge-transfer coefficient

η^r is the local overpotential

j_0^r is the exchange-flux density

$k_{\text{norm},0}^r$ is a reaction-rate constant

R_f^r is the resistivity of the surface film that may exist on the electrode particles

This equation is valid for the negative- and positive electrode regions and is a good description of reaction kinetics for constant-current events, but misses some critical cell behaviors at high frequencies.

The electrochemical mechanism model can comprehensively describe the process changes of battery operation, which is of great significance for battery design and optimization. At the same time, it is very helpful for analyzing remaining capacity, predicting battery service life, analyzing electrochemical performance, and electric thermal coupling. Its model is often used as a benchmark for verification and comparative analysis in lithium-ion battery research due to its high accuracy. However, the model contains a coupled nonlinear partial equation system, which makes the solution and calculation more complex and expensive, and is not suitable for real-time computing applications. Although there have been numerous studies simplifying their complex models to improve computational speed and stability, there are still limitations to each. Therefore, the development of electrochemical modeling methods with high computational efficiency, good accuracy, and wide applicability still needs further research.

Table 2 Comparison of various Electrochemical models of battery

Model	Merits	Demerits
Extended single particle (ESP) Model	The electrode is reduced to a single active particle. PDEs are solved using approximate solution method or curve fitting. Increases the effectiveness of computation.	The complexity of the model rises
Reduced order Model or Single Particle (SP) Model	Simple model that reduces the electrode to a single particle and ignores the liquid phase	The solid-phase Li-ion concentration in the SP model still requires the solution of radial-domain PDEs. Precision at high C-rates is lacking
	High accuracy	High computational complexity

2.2. Equivalent Circuit Model

The equivalent circuit model uses traditional circuit components such as resistors, capacitors, and constant voltage sources to form a circuit network to describe the external characteristics of power batteries. This model uses a voltage source to represent the thermodynamic equilibrium potential of the power battery and an RC network to describe the dynamic characteristics of the power battery. Compared with the electrochemical model of lithium-ion batteries, the equivalent circuit model achieves a compromise between model complexity and accuracy, has good practicality for various working states of power batteries, and can derive the state equation of the model for analysis and application. The modeling of equivalent circuit models has been extensively studied and developed in battery management applications, including time-domain analysis methods based on voltage and current data and frequency-domain analysis methods based on impedance spectra. The common equivalent circuit models for power batteries include the Rint model, Thevenin model, PNGV, and Dual Polarization (DP) model[18], which are special cases of the n/RC equivalent circuit model at $n=0$, $n=1$, and $n=2$, respectively[19][20][21]. Impedance spectrum models, non integer order equivalent circuit models, and improved models. The following will describe the n/RC equivalent circuit and impedance spectrum model. Figure 5 shows a typical equivalent circuit model of a power battery composed of n RC networks, abbreviated as n-RC model

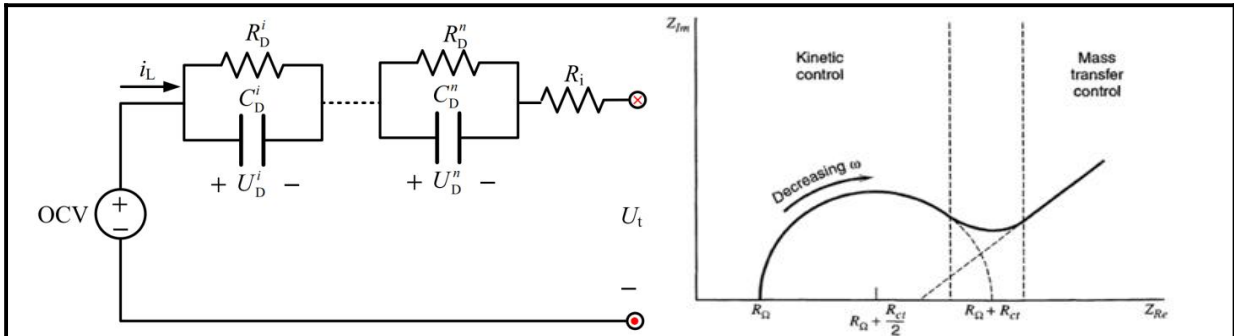


Figure 6. Lithium battery n-RC model and Electrochemical impedance spectroscopy

This model consists of three parts: voltage source: using open circuit voltage UOC to represent the open circuit voltage of the lithium battery; Ohmic resistance: R_i is used to represent the electrode material, electrolyte, diaphragm resistance, and contact resistance of various components in lithium batteries; RC network: describes the dynamic characteristics of lithium batteries, including polarization characteristics and diffusion effects, through polarization internal resistance R_D^i and polarization capacitance C_D^i , where $i=1, \dots, n$.

Electrochemical Impedance Spectroscopy (EIS) is a typical method for solving equivalent circuit parameters. By comparing the model expression of the battery equivalent circuit in the frequency domain with the measured impedance data, the parameter values of the model are obtained by fitting. [22]

Figure 5 shows the electrochemical impedance spectroscopy test results of lithium battery cells. The various parts of the equivalent circuit of lithium-ion batteries based on EIS are often related to specific electrochemical reaction processes. The main resistance represents the conductivity of the electrolyte, separator, and electrode, the charge transfer resistance and double-layer capacitance describe the activation polarization voltage drop, and the constant phase Warburg element characterizes the diffusion effect of lithium ions inside the battery. The frequency part is a semicircle with a center located below the horizontal axis, which is generally believed to be related to the double layer at the interface between the electrode and the electrolyte. When fitting this characteristic, researchers have found that equivalent circuit models using pure capacitive components often fail to achieve ideal fitting accuracy. The phenomenon of inconsistency between the experimentally measured double-layer frequency response characteristics and pure capacitance is called the "dispersion effect". This deviation from pure capacitance can be fitted by a constant phase angle element. EIS model can reflect the physical and chemical changes inside the battery and the mapping of circuit components; EIS relies on SOC, current, temperature, and SOH, which increases the complexity of the model, but sometimes considering these effects through model fusion becomes an advantage. Using impedance expressions with fractional order to fit the EIS of batteries based on the characteristics of EIS can obtain non integer order models [23][24][25]

Based on the equivalent circuit modeling described in existing literature, different research focuses have their own advantages, but this also brings about differences in accuracy. Models with fewer circuit components and simpler structures consider limited factors that affect battery dynamic characteristics, resulting in poor accuracy; However, as the factors considered increase, the accuracy is also enhanced, but at the same time, it also brings the disadvantage of complex models that are not conducive to real-time computing applications. The equivalent circuit model based on fractional order and battery EIS has a relatively simple structure and can better describe the dynamic characteristics of the battery. Compared with ordinary integer order equivalent circuit models, the model is more concise and can reflect more

dynamic characteristics with relatively equal accuracy. The measurement of battery EIS usually requires expensive equipment, and repeated tests are required to determine model parameters, which makes it difficult to adjust the fractional order model with the aid of EIS research in application. The related theoretical methods and application research of equivalent circuit model based on fractional order still need to be further deepened.

2.3. Data driven model

Due to the complex internal principles of batteries and uncertain working conditions, it is difficult to establish a model that accurately reflects the dynamic characteristics of batteries. The data-driven battery modeling method considers the battery as a "black box model" and constructs a training sample set using the excitation input, response output, and other parameters of the battery under different conditions to train data-driven black box models that reflect the linear and nonlinear relationships between battery input and output and other parameters. Typical examples include artificial neural networks (ANNs), fuzzy logic models, and support vector machine (SVM) models. A neural network-based thermoelectric coupling model has been verified through different battery tests. Fuzzy model of a battery using Mamdani and Sugeno methods and electrochemical impedance based test data.

Based on the data-driven models reported in existing literature, it is analyzed that although artificial neural network models can effectively work under the nonlinear conditions of batteries, they require a massive amount of data to train the model; When using a typical training sample set, the fuzzy logic control model can approximate nonlinear conditions, but it also requires a large amount of data and complex calculations; The support vector machine model transforms a low dimensional nonlinear model into a high-dimensional linear model based on kernel functions. After training with appropriate sample data, it can accurately predict the capacity state of the battery. The appropriate sample data and training calculation time are important factors affecting accuracy. Data driven models based on training samples require careful training and validation, and the typicality and completeness of the training sample set directly affect the accuracy of the training model due to factors such as battery variability, working environment conditions, diverse operating conditions, and aging.[26]

The data-driven battery modeling method can achieve high-precision simulation for battery characteristics, thereby obtaining a higher SoC estimation accuracy. The training and updating of the model requires large amount of computing resource and time, which makes it impossible to be applied in V-BMS. To improve the accuracy and stability of battery modeling and SoC estimation while ensuring the system real-time performance, a conjunction working mode between C-BMS and V-BMS was proposed in[28] as shown in **Figure 7**.

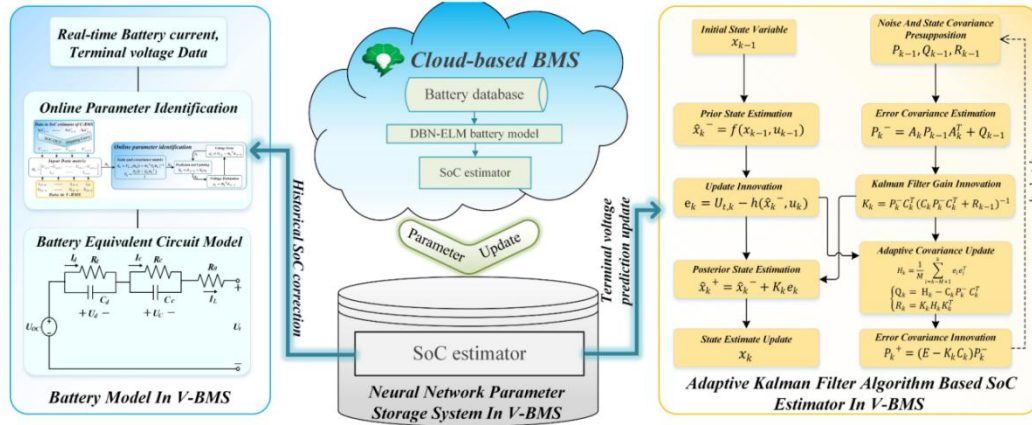


Figure 7. Lithium-Ion battery(LIB) State of Charge(SoC) estimaion method based on the conjunction between Cloud based Battery Management System(C- BMS) and Vehicle based Battery Management System(V- BMS) schematics using Equivalent Circuit Model(ECM) in Battery Modelling with Adaptive Kalman Filter (AKF) for SoC estimation in V-BMS and Neural Network parameter Storage System in V-BMS, while Deep Belief Network Extreme Learning Machine(DBN-ELM) in C-BMS[28]

2.4. Battery state estimation method

The estimation of battery state (SOX, including SOC, SOH, SOP, etc.) is one of the core functions of energy storage battery management systems. Accurate SOX estimation can ensure the safe and reliable operation of power battery systems, optimize power battery systems, and provide a basis for energy management and safety management.

2.4.1. State of Charge (SOC)

State of Charge (SOC), as one of the important decision-making factors in energy management, plays a crucial role in optimizing the energy management of the entire system, improving the capacity and energy utilization efficiency of lithium batteries, preventing overcharging and overdischarging of batteries, and ensuring the safety and longevity of lithium batteries during use.

The internal structure of lithium batteries is complex, and the electrochemical reaction process and stages are complex and difficult to determine. Sometimes, the working conditions are harsh and varied, and it is difficult to obtain the accurate value of SOC as an implicit state variable. Common methods for estimating SOC of lithium batteries can be roughly divided into four categories: methods based on characterization parameters, ampere hour integration methods, model-based methods, and data-driven methods. As shown in **Figure 8** below

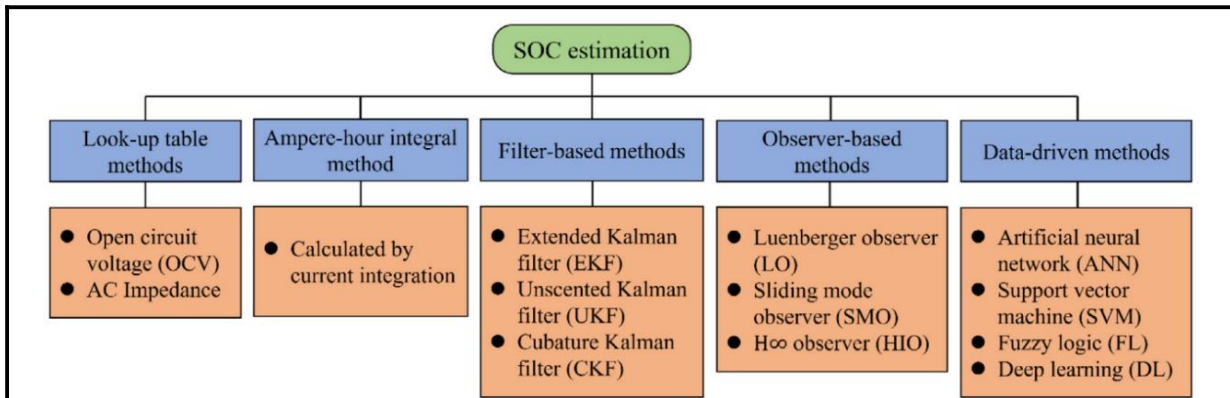


Figure 8. SoC estimation method for lithium ion batteries[26]

The Ampere hour integral method is the simplest and most widely used engineering estimation method for State of Charge (SOC). When the accuracy and sampling frequency of the sensor meet certain requirements, and the initial SOC is accurate, this method has good estimation accuracy. However, the accuracy of current sensors, especially drift noise, will lead to error accumulation effects, affecting the estimation accuracy of SOC. Therefore, this method is difficult to meet the high accuracy requirements for SOC estimation. Due to the correlation between SOC and the amount of lithium ion active material embedded, and the open circuit voltage of lithium batteries reflecting the voltage at ion balance inside the battery, the open circuit voltage method is an effective SOC estimation method. However, this method requires the battery to be left idle for a long time, so it is only suitable for laboratory estimation and not for online estimation during battery use. The neural network method utilizes the nonlinear mapping characteristics of neural networks and is a universal and suitable estimation method for various batteries. The disadvantage of this method is that it requires a large number of training samples, and the difference between training samples and training methods can affect the accuracy of estimation. On the other hand, the neural network method requires a large amount of computing resources, which requires powerful processing chips. In recent years, model-based estimation methods have been widely used due to their advantages such as easy identification of model parameters and strong disturbance resistance. G. L Plett proposed using different battery models combined with Extended Kalman Filter (EKF) to estimate the state of charge of batteries. However, traditional EKF also has some drawbacks: firstly, this method relies heavily on model accuracy. Secondly, system noise and observation noise must follow a Gaussian distribution, otherwise the performance of the filter will be reduced, and even differentiation may occur. Xiong Rui, He Hongwen, and others from Beijing Institute of Technology [59-61] used an improved adaptive extended Kalman filter to estimate the SOC of batteries, overcoming the aforementioned drawbacks. References [62-65] applied Particle Filter (PF) to SOC estimation and achieved good estimation accuracy.

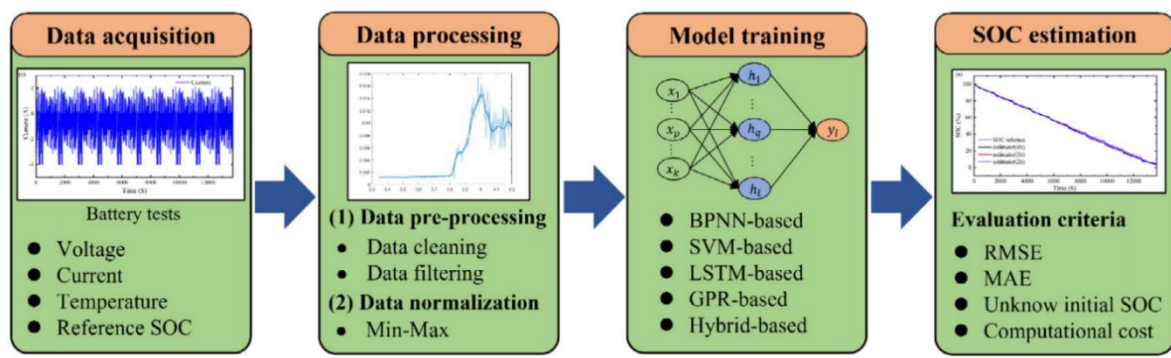


Figure 9 The procedures for developing ML SOC estimation Algorithms[26]

2.4.2. State of Health (SOH)

Accurately assessing the health status of batteries is of great significance in ensuring the safe operation of energy systems and avoiding potential failures. With the extension of battery life, the ability to store energy and provide a certain amount of power will decrease due to aging. Therefore, State of Health (SOH), as an important indicator for evaluating battery aging status, is crucial for safe operation. Once the health indicators reach the predetermined limits, the battery should be removed from the energy storage system. From the study of internal aging mechanisms of different battery types, lithium content loss, active material decomposition, and structural changes are common causes of capacity loss. The increase in resistance is mainly due to the growth of the solid electrolyte interface (SEI) layer. According to the battery testing procedure manual, under a specific testing plan, when the battery capacity drops to 80% of the initial rated capacity, it is considered unsuitable for use and needs to be replaced. But in some cases, an increase in internal resistance leads to a significant decrease in power, which can cause the battery to fail prematurely. Therefore, considering both aspects comprehensively is crucial for the normal operation of the energy system. The significant changes in the characteristics of batteries during aging also indicate an increase in the possibility of battery failure, such as charging curves, OCV (open circuit voltage) curves, etc. [70-72]. Considering the online and simple implementation requirements of practical applications, many works focus on model-based methods using different estimation techniques.

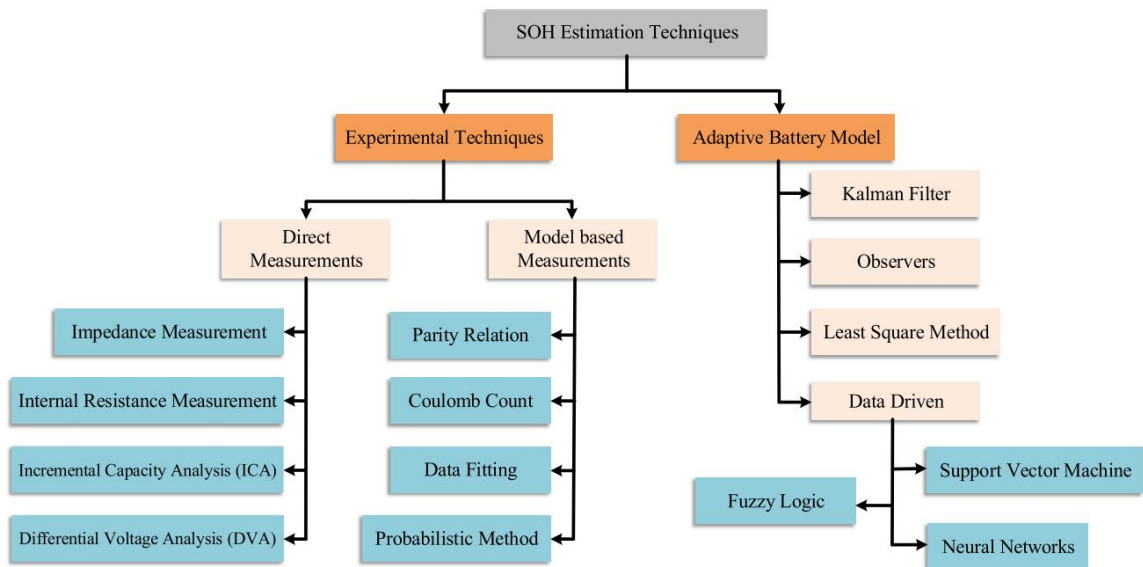


Figure 10. SOH estimation method for lithium batteries

As an indispensable technology in BMS (Battery Management System), various tools and methods have been extensively studied for SOH estimation. However, from estimating health-related features to estimating the overall SOH of lithium batteries, it remains a very challenging task. Due to the many factors that affect the aging process of batteries, such as temperature and charge discharge rate, studying the aging laws under these factors requires long-term cycling tests and characteristic experiments. Although most methods have been fully validated in a large amount of experimental data, the feasibility and reliability of these methods in practical situations still need further discussion.

Different literature has proposed different SOH classifications based on their respective characteristics. In order to track these degradation behaviors in BMS, battery estimation methods are divided into two categories: experimental methods and model-based estimation methods. Each branch contains several common methods, as shown in the above figure. Although a large number of SOH estimation methods have been studied, each method has its shortcomings and potential for improvement, and further research and experimentation are needed in conjunction with engineering and work conditions.

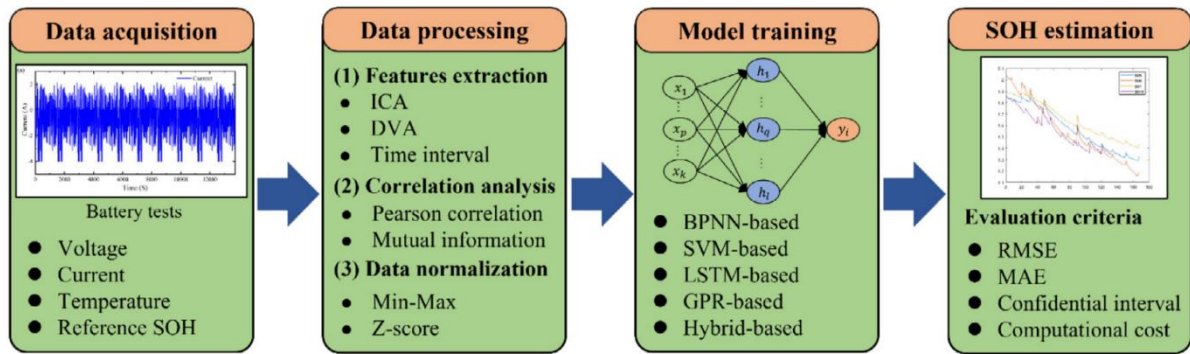


Figure 11 The procedures for developing ML SOC estimation Algorithms[26]

3. Research content of thesis

The main theories, research methods, specific technical routes, and implementation plans to be adopted in this paper are as follows:

3.1. Modeling, parameter identification, and joint estimation of SOC and SOH for lithium battery

A battery model attempts to emulate the behavior of a battery as close to reality as possible. The model allows computing directly unmeasurable states of the battery, such as SOC, SOH, TTS, and RUL (see Figure 3.2). Based on these computed states, the BMS issues electronic control signals to maintain the state of the battery at favorable levels. Present-day battery models are very reliable to predict instantaneous states of the battery, such as SOC, state of power, and TTS. Models to predict the accumulative states of the battery, such as power fade, capacity fade, SOH, and RUL, are still in the early stages.

3.2. Equivalent circuit model

Two different equivalent circuit models are presented and discussed: the direct current (DC) equivalent circuit model and the alternating current (AC) equivalent circuit model.

Figure 13 shows the DC equivalent circuit model (DC-ECM) of a battery. The electromotive force of the battery is denoted by EMF, $h(k)$ denotes hysteresis, R_0 , R_1 , R_2 denote ohmic resistance, and C_1 , C_2 denote capacitance. The voltage across the battery terminals and the current through the battery is denoted by $v(k)$ and $i(k)$, respectively. The current through resistances R_1 and R_2 are denoted by $i_1(k)$ and $i_2(k)$, respectively. This makes the current through capacitances C_1 and C_2 to be $i(k) - i_1(k)$ and $i(k) - i_2(k)$, respectively. Here, the time is denoted in discrete domain (i.e., $i(k)$ denotes the current measured at time (k)). Based on the notations described so far, and shown in Figure 15, the measured voltage across the battery terminals can be written as

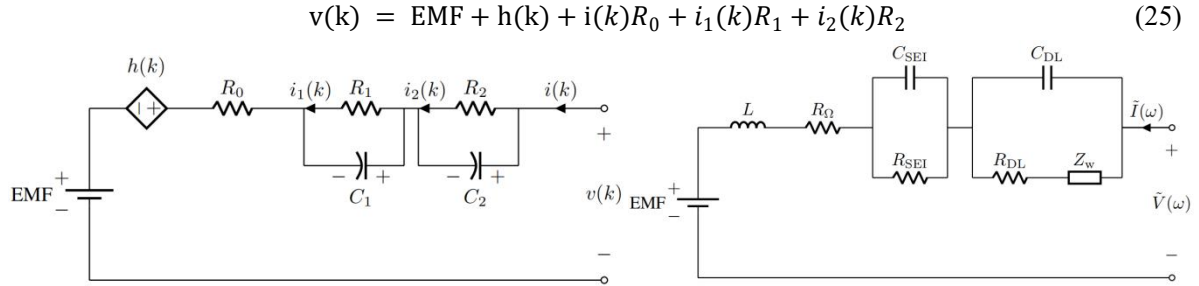
$$v(k) = \text{EMF} + h(k) + i(k)R_0 + i_1(k)R_1 + i_2(k)R_2 \quad (25)$$


Figure 12 DC equivalent circuit model and AC equivalent circuit model.

The currents $i_1(k)$ and $i_2(k)$ can be derived in terms of $i(k)$ as follows

$$i_1(k+1) = \alpha_1 i_1(k) + (1 - \alpha_1) i(k) \quad (26)$$

$$i_2(k+1) = \alpha_2 i_2(k) + (1 - \alpha_2) i(k) \quad (27)$$

where $\alpha_1 = e^{-\frac{\Delta}{R_1 C_1}}$, $\alpha_2 = e^{-\frac{\Delta}{R_2 C_2}}$ and Δ denotes the sampling time. The quantities R_1 , R_2 , C_1 and C_2 , in Figure 15 are shown without a time index (k) , indicating that these are the ECM parameters. Hysteresis is shown with time index (k) , indicating that hysteresis is not a constant parameter; rather, it is a quantity that changes with time.

The AC equivalent circuit model of the battery that is also known in the literature as the adaptive Randles equivalent circuit model (AR-ECM). In addition to the EMF component, the AR-ECM consists of the following elements: stray inductance L , ohmic resistance R_Ω , solid electrolytic interface (SEI) resistance R_{SEI} , solid electrolytic interface (SEI) capacitance C_{SEI} , double layer (DL) resistance R_{DL} , double layer (DL) capacitance C_{DL} , and Warburg impedance Z_w .

The AC and DC equivalent models are very similar as they both represent the same battery. One significant exception in the AC equivalent circuit model is the Warburg impedance, denoted as Z_w in **Figure 13**. The Warburg impedance is written as

$$Z_w \triangleq Z_w(j\omega) = \sigma \sqrt{\frac{2}{j\omega}} \quad (28)$$

where ω indicates angular frequency. It can be noticed that the Warburg impedance is significant only at

very low frequencies. At high frequencies (i.e., when ω is significantly high), the effect of Warburg impedance becomes insignificant and the AC equivalent circuit starts to look very similar to its DC counterpart. The expression for Warburg impedance in (28) is only an approximation.

Let us denote the voltage across the battery and the current through it as

$$V(\omega) = V_{dc} + \tilde{V}(\omega) \quad (29)$$

$$I(\omega) = I_{dc} + \tilde{I}(\omega) \quad (30)$$

where $V(\omega)$ and $I(\omega)$ denote the voltage and current measurements consisting of the DC component (V_{dc} , I_{dc}) and AC component ($\tilde{V}(\omega)$, $\tilde{I}(\omega)$). The AC impedance of the battery can be written as

$$\begin{aligned} Z(j\omega) &= \frac{\tilde{V}(\omega)}{\tilde{I}(\omega)} = j\omega L + R_{\Omega} + \frac{1}{\frac{1}{R_{SEI}} + j\omega C_{SEI}} + \frac{1}{\frac{1}{R_{CT} + Z_w(j\omega)} + j\omega C_{DL}} \\ &= j\omega L + R_{\Omega} + \frac{R_{SEI}}{1 + j\omega R_{SEI} C_{SEI}} + \frac{R_{CT} + Z_w(j\omega)}{1 + j\omega (R_{CT} + Z_w(j\omega)) C_{DL}} \end{aligned} \quad (31)$$

By measuring the AC impedance across a battery, the AR-ECM model parameters can be estimated. Such frequency-domain impedance analysis is known as electrochemical impedance spectroscopy (EIS).[\[27\]](#)

3.3. Deep Learning framework overview

The limitations of existing SOC estimation methods motivate the battery community to develop more accurate and efficient SOC estimation methods. The fast development of artificial intelligence has accelerated the popularity of data-driven SOC estimation. The promising applications of machine learning in the estimation of SOC and state of health (SOH) for batteries could be the future.

Machine learning techniques include linear regression, random forest, support vector machine, Gaussian processes and neural networks. A data-driven framework based on deep learning for estimating SOC and SOH, which mainly consisted of long short-term memory (LSTM) neural network and back propagation neural network.

Deep learning, represented by deep neural networks (DNNs), has become a game changer in many fields, such as computer vision and natural language processing. As the DNNs can carry out end-to-end learning by automatically learning all steps between the initial input and the eventual output, the reliance on expert knowledge or feature engineering can be significantly eased. Recently, deep learning has spurred innovation in the field of battery management. Deep learning-based SOC estimation methods can directly map sampled battery operating signals (e.g., current and voltage) to SOC. Therefore, arduous battery modelling or feature engineering is no longer needed. In addition, deep learning methods have high scalability, which allows training models based on large datasets coming from different types of batteries. In the era of big data where massive battery operating data are collected, deep learning methods become a promising alternative and are expected to bridge the gap between the surge of battery big data and the limited learning ability of conventional SOC estimation methods. Recent studies have substantiated the efficacy of deep learning methods under various challenging conditions, even in the presence of low SOC, low temperatures and voltage plateaus.

3.3.1. State of charge estimation

Battery SoC is defined as

$$SOC_t = \frac{Q_t}{Q_{max}} \quad (32)$$

where Q_t represents the available capacity at the time instant t and Q_{\max} represents the maximum capacity, which can be obtained through measurement or estimation. Since SoC is not directly measurable, a battery management system (BMS) attempts to use the sampled current, voltage and other signals (e.g., surface temperature) to determine SOC. As shown in Fig. above, deep learning methods establish a nonlinear mapping between the measured signals and SOC in an end-to-end manner. Without losing generality, we take the most frequently used voltage and current data as an example. At the time instant t , the voltage and current sequences are collected in a window with the length of T , which are then fed into a DNN to estimate

$$\begin{cases} x_1 = [V_t \ L_t] \\ \hat{z}_t = f_{DNN}(x_{t-T+1:t}) \end{cases} \quad (33)$$

Where V , I and \hat{z} represent voltage, current and the SOC estimation result and $x_{t-T+1}, x_{t-T+2} \dots x_t$ represents the input sequence f_{DNN} stands for mapping between the input and output

3.3.2. Framework of deep learning based SOC estimation

In contrast to conventional model-based methods which establish the mapping by resorting to physics-based models, deep learning methods provide a convenient approach to learning the mapping from vast training data. Specifically, deep learning uses a deep structure to learn hierarchical representations from training data [25]. This process is generally fulfilled by neural networks because of their flexible structure.

In general, the deep learning-based SOC estimation includes data generation, model development and model deployment as shown in **Figure. 14**.

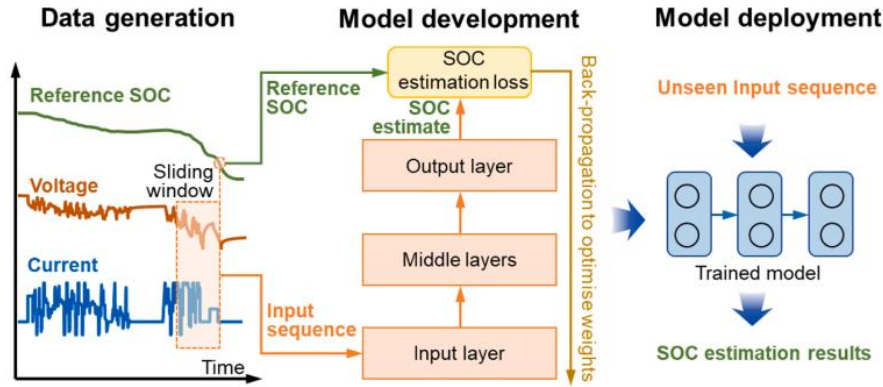


Figure 13 Structure and training strategy of a deep neural network for SOC estimation.

3.3.3. Data generation:

As a data-driven approach, DNNs rely on a training dataset to learn the mapping described in Eq. (33). A training dataset accommodates the voltage and current data collected from battery operations. The reference SOC is computed by resorting to Ampere-hour counting. In the context of battery testing, high-accuracy battery test equipment and a regulated testing environment can ensure accurate current sampling. In addition, the initial SOC can be accurately determined by fully charging/discharging the batteries to the upper and lower voltage limits, which correspond to the SOC of 100% and 0, respectively. Then, the current and voltage data can be sliced together with reference SOC to support the supervised

training of a DNN. The training data are expected to cover wide SOC ranges, and the current and voltage profiles are expected to reflect realistic battery usage. Existing training datasets can be classified into two types, namely static and dynamic datasets. The static dataset considers the battery SOC estimation under a controllable condition to rule out the impact of unseen current excitations. For instance, battery charging is controllable in many scenarios. In view of this, Tian et al. investigated the SOC estimation during the constant-current constant-voltage (CCCV) charging, which is a prevalent battery charging protocol adopted in electric vehicles (EVs). A DNN was adopted to map the current and voltage sequence to the SOC according to Eq.(2). Once the SOC is estimated at the constant-current charging stage, the SOC is propagated based on Ampere-hour counting until the next charging stage. Hu et al. extended this kind of method from the CCCV charging to additional four advanced charging protocols, including multistage constant current constant voltage (MCCCV), constant power constant voltage (CPCV), alternating current (AC) and pulse charging (PC). The results demonstrate the effectiveness of the DNN-based SOC estimation under various charging conditions. The dynamic datasets represent more general cases where the batteries operate under dynamic current excitations. Such cases are prevalent in many new-energy energy storage scenarios, such as photovoltaic systems where energy generation and consumption are both dynamic.

3.3.4. Model development:

DNN can be established to learn the mapping described in Eq. (2) from the training dataset. As shown in Fig. 2, a DNN consists of an input layer, multiple middle layers and an output layer. The stacked layers incorporate representation learning and sequential data regression, offering high flexibility in handling various types of data. In this regard, the model performance heavily depends on the layer and model structures. In addition to the basic DNN with the fully connected layers, advanced layers with powerful feature extraction abilities have been developed by the deep learning community. For example, the convolutional layer, inspired by findings in terms of biological vision, provides state-of-the-art performance for image processing. The recurrent neural network (RNN) layers can accommodate the sequence-dependent data and have demonstrated their efficacy for speech recognition. The working principles and applications of different types of DNNs are discussed in Section 3 to clarify their performance in terms of SOC estimation. Once a DNN is developed, it is usually parameterised in a supervised fashion. Weights in each layer are optimised by minimising the discrepancy between the SOC estimate and experimentally obtained

$$\theta_{DNN} \argmin f_{loss}(z, \hat{z}) \quad (34)$$

where z and \hat{z} are the reference SOC and estimate, respectively. f_{loss} is the loss function measuring the difference between the estimation results and reference.

In the context of battery SOC estimation, a variety of loss functions can be adopted, such as the mean squared error (MSE) and mean squared error (MAE). The minimisation problem is addressed through backpropagation, i.e., parameters are updated using the following rule

$$\theta_{DNN} \leftarrow \eta \frac{\partial f_{loss}(z, \hat{z})}{\partial \theta_{DNN}} \quad (35)$$

Where η denotes learning rate

3.3.5. Model deployment:

The trained DNN model can be deployed in a BMS to estimate SOC from pieces of voltage and current data. The estimation results can serve as the basis for other battery management tasks such as battery charging and fault diagnosis.

Table 3 Summary of the applications of hybrid algorithms for state estimation.[26]

Fusion Type	Hybrid Method
The fusion of model-based and ML methods	BPNN + EKF
	RBFNN + UKF
	ELM + AUKF
	DNN + UKF
	NARX + UKF
	LSTM + SPKF, LSTM + ACKF, LSTM + PF
	GPR + RLS
The fusion of different ML methods	LR + RBFNN
	CNN + GRU
	CNN + LSTM
	CNN + 2D CNN
	LR + GPR

Table 4 Summary of the publicly available battery datasets. [26]

Sources	Reference
Panasonic NCR18650PF LiBs	[29]
LG 18650HG2 LiBs	[30]
LFP A123(APR18650M1A) LiBs	[31]
Center for Advanced Life Cycle Engineering (CALCE) at the University of Maryland	[32]
Research & development data repository from Sandia National Labs	[33]
NASA Ames Prognostic Data Repository	[34]
Oxford battery degradation dataset from Howey research group	[35]

4. Preliminary Work Research plan and outcome

4.1. Research plan and outcome

Table 5 Research planing and work content

Research Plan	Starting and ending dates	Completed content
	2024.9-2025.1	Literature review, research topic selection and proposal report
	2024.2-2025.3	Online dataset collection and experimental dataset collection using battery cycling, Electrochemical Impedance Spectroscopy(EIS) measurement of selected cells and preparation for modelling
	2025.4-2025.05	Modeling, parameter identification, and SOC/SOH joint estimation research using Equivalent Circuit Model and data driven methods for lithium batteries
	2025.06-2025.07	Use the State of art technique for battery modelling based on physics and electrochemistry such as P2D, SPM, SPMe for comparion with developed model using ECM and machine learning
	2025.08-2025.09	write the graduation thesis and prepare for final defense

4.2. Thesis Objectives and Contributions

The main goal of the thesis is to build a simulation framework for BEVs and their main energy source batteries, which can estimate battery performance and life under given driving and usage conditions.

The key contributions of this thesis are concentrated on the following to achieve the goals:

A. Constructing three different battery modeling approaches:

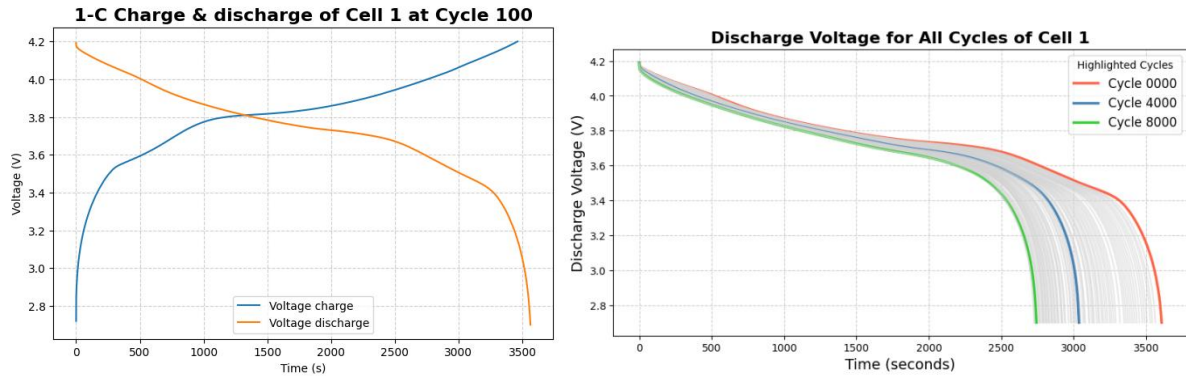
- (1) An empirical model which is known as ECM consist of circuit elements such as resistors and capacitors
- (2) Data driven Model that depend on data collected in the lab and under usage for better prediction of battery ageing mechanism in combination with physics based approach using SPMe.

B. Building a simulation environment for an electric vehicle in Matlab/Simulink and integrating it with the battery models in Matlab for BEV simulation, which can take driving profile and ambient temperature as an input and provides battery states SOC, SOH, etc as an output.

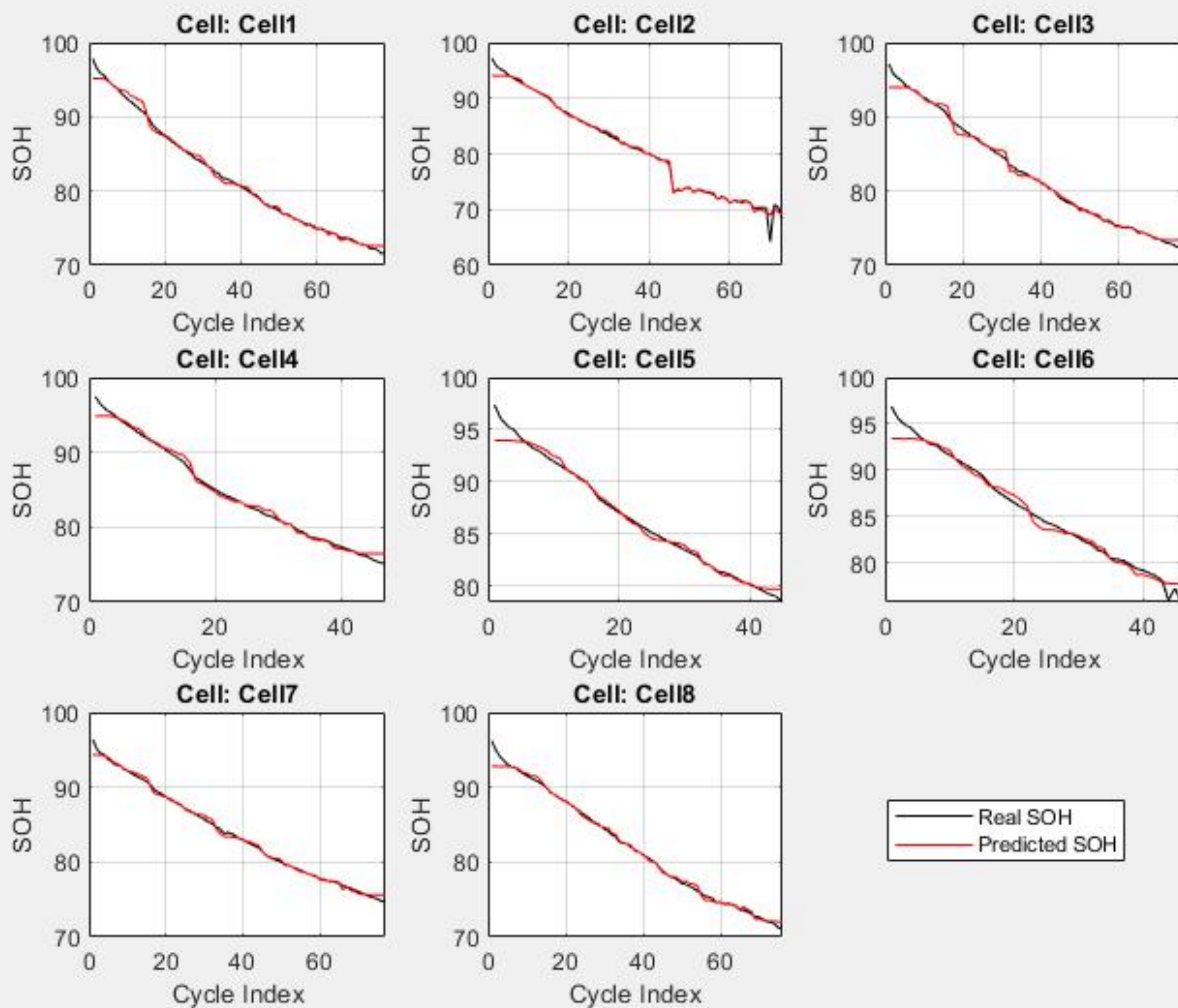
C. Accuracy comparison of 1-RC model, 2-RC model and Various Deep Learning algorithms such as FFNN, LSTM, and implementation of the hybrid methods such as LSTM + SPKF, LSTM + ACKF, LSTM + PF etc

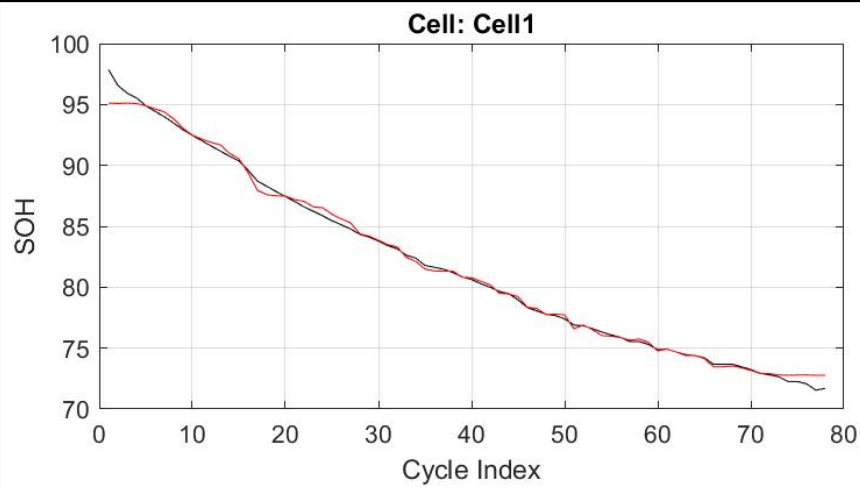
5. Preliminary Work

5.1. Oxford Battery Dataset analysis for SoH estimation using Linear Regression, Random Forest Regressor and Support Vector machine , :

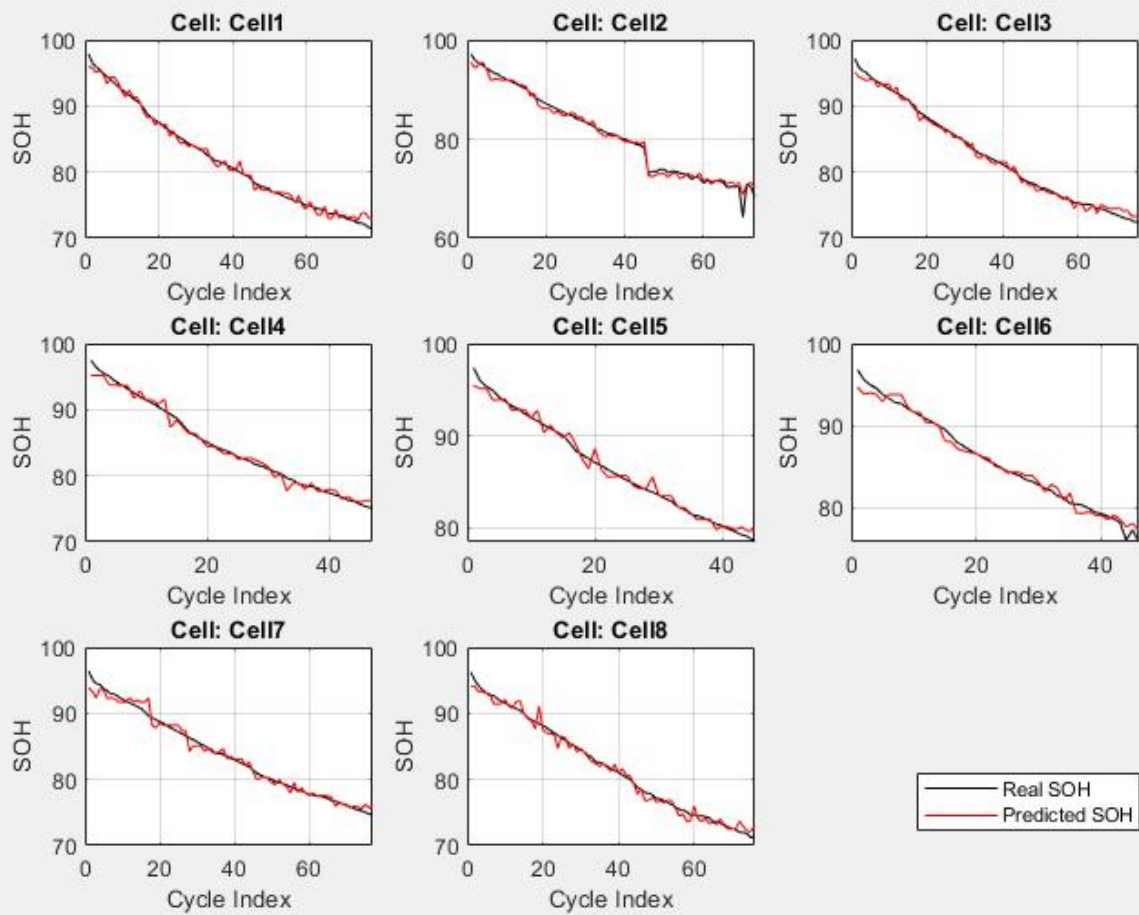


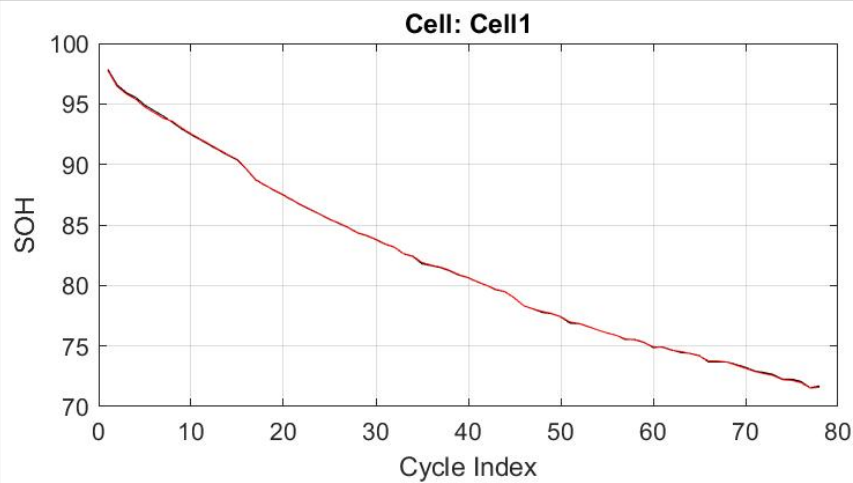
Extremely Randomized Tree Regressor(ERTR)





K-nearest Neighbor regressor





5.2. NASA battery dataset analysis for SoH estimation using DNN

Training set of battery B0005

Validation with B0006

The following graph illustrates the battery aging process as the charge cycles progress. The horizontal line represents the threshold associated with what is considered the end of the battery's life cycle.

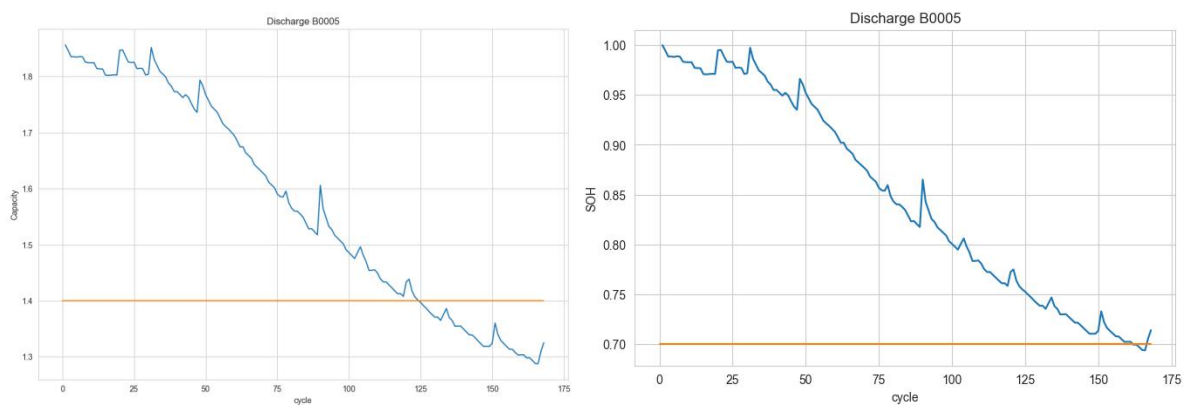


Figure 14 Discharge of B0005 cell showing Capacity Ah (left) and SoH %(right)

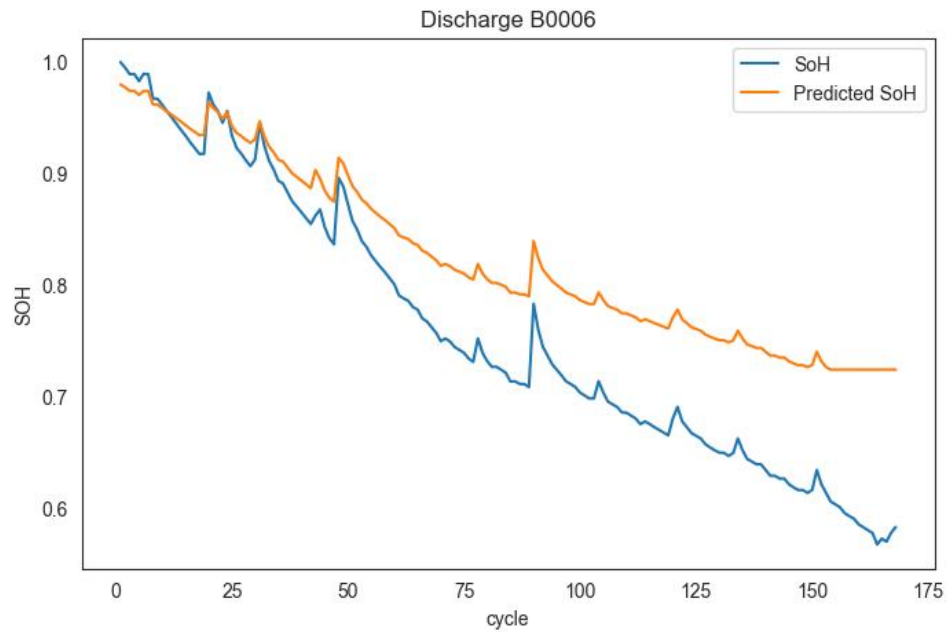
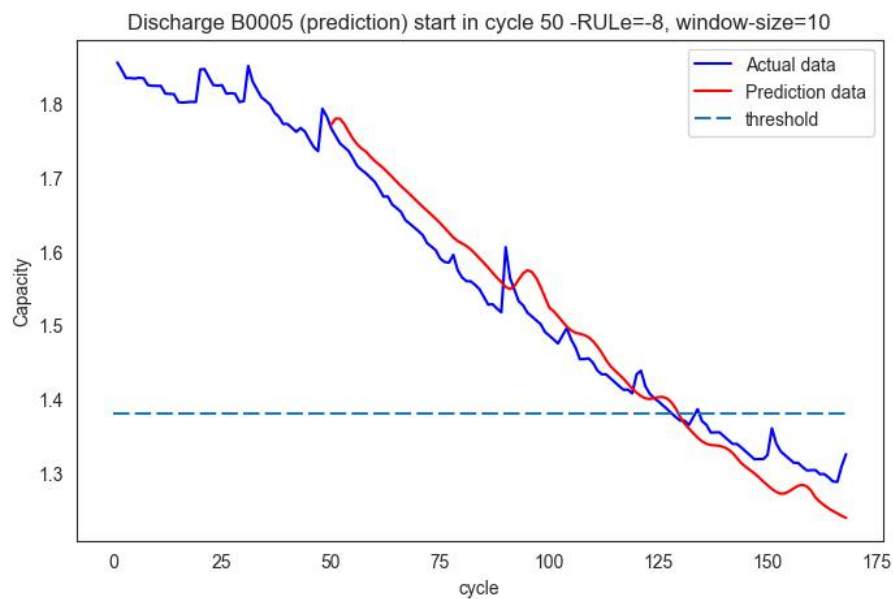


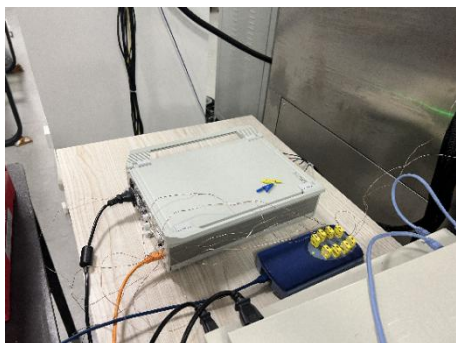
Figure 15 To visualize and compare the differences between the actual and predicted State of Health (SoH), we can plot both sets of values on the same graph. This will help in evaluating how well the model has performed in predicting the SoH for the test battery (B0006).



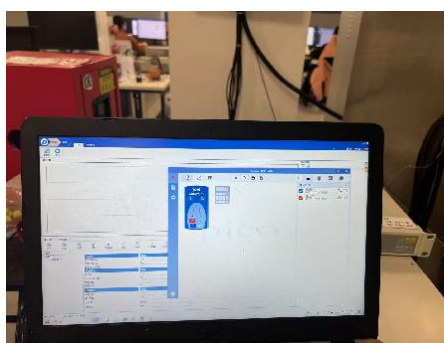
Remaining useful life prediction
[37][38][39]

5.3. Electrochemical Impedance Spectroscopy test experiment in at varying temperature:

Experiment equipments:



EIS test equipment



Data acquisition computer



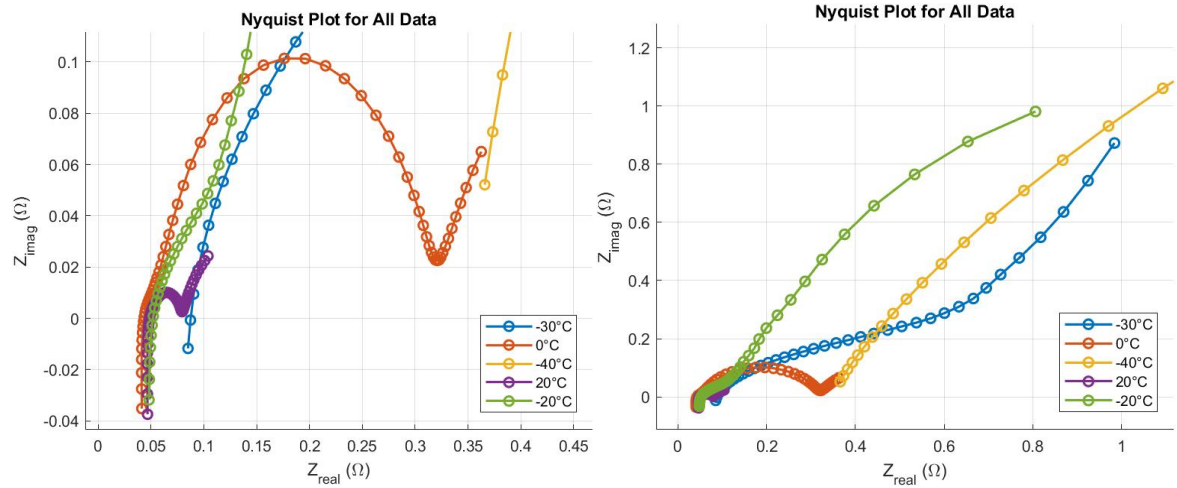
Temperature controlled chamber



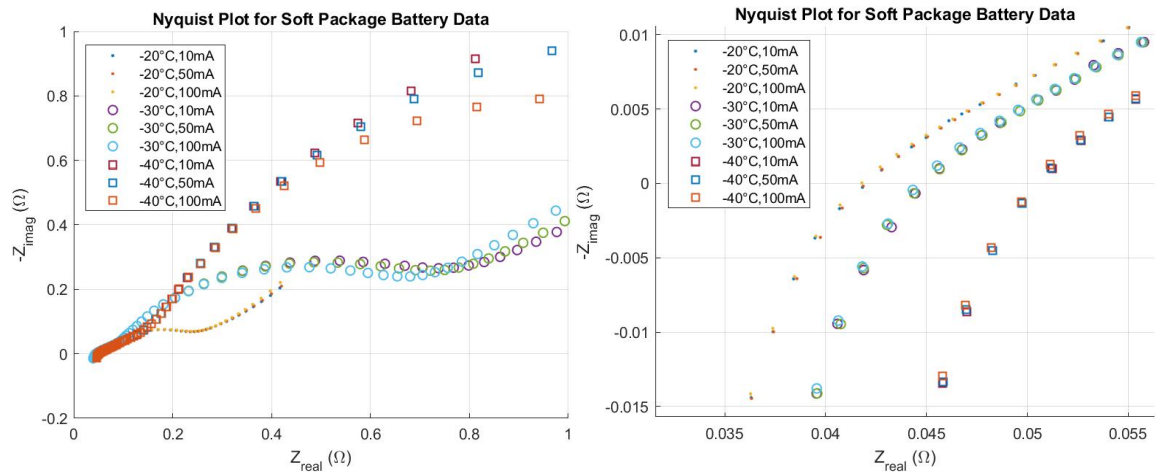
6000 mAh pouch cell

5.3.1. LiFeSO₄ Cylindrical cell EIS test in temperature variation





5.3.2. Pouch Cell :



5.3.3. Result

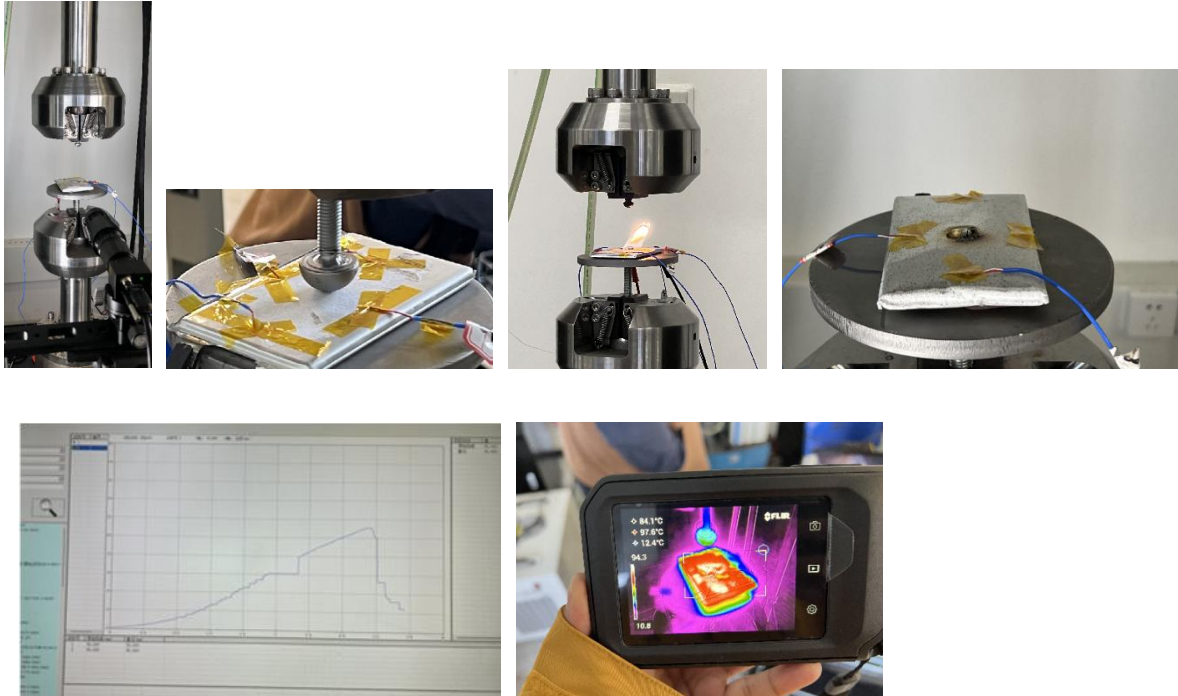
Cylindrical Cell

Cell performs well at 20 degrees and even in 0 degrees but poorly in -20 degrees and below

Pouch Cell

Cell performs well at -20 but poorly in -30 Degrees and -40 Degrees

Other works - Battery thermal performance test under stress environments



6. Conclusion

- Relevant literature review of various battery modelling techniques
- BMS is responsible for better battery performance, longevity, and protection from damage.
- Equivalent circuit model is the most famous and widely used battery modelling technique.
- Electrochemical model can produce high accuracy state prediction with various internal cell parameters but it is computationally expensive and fairly difficult to start.
- Data driven battery modelling technique is also known as 'black box model' but shows promising results. It offers easy to start modelling but highly dependent on training data from experiments.
- Thus, lots of experiments like battery cycling, Electrochemical Impedance Spectroscopy are needed to model the commercially available Lithium ion batteries.
- Focus on developing accurate Data Driven Model and implement in Matlab/simulink environment for EV simulation considering different driving profiles and ambient temperatures

7. References:

- [1] C. McGlade and P. Ekins, "The geographical distribution of fossil fuels unused when limiting global warming to 2 °C," *Nature*, vol. 517, no. 7533, pp. 187–190, Jan. 2015. doi:10.1038/nature14016
- [2] N. Armaroli and V. Balzani, "The future of energy supply: Challenges and opportunities," *Angewandte Chemie International Edition*, vol. 46, no. 1–2, pp. 52–66, Dec. 2006. doi:10.1002/anie.200602373
- [3] Peralta P., C., Vieira, G.T., Meunier, S., Vale, R.J., Salles, M.B., & Carmo, B.S. (2019). Evaluation of the CO2 Emissions Reduction Potential of Li-ion Batteries in Ship Power Systems. *Energies*.
- [4] D. Stampatori, P. P. Raimondi, and M. Noussan, "Li-Ion Batteries: A Review of a Key Technology for Transport Decarbonization," *Energies*, vol. 13, no. 10, p. 2638, May 2020, doi: 10.3390/en13102638.
- [5] R. R. Kumar, C. Bharatiraja, K. Udhayakumar, S. Devakirubakaran, K. S. Sekar, and L. Mihet-Popa, "Advances in Batteries, Battery Modeling, Battery Management System, Battery Thermal Management, SOC, SOH, and Charge/Discharge Characteristics in EV Applications," *IEEE Access*, vol. 11, pp. 105761–105809, 2023, doi: 10.1109/ACCESS.2023.3318121.
- [6] V. A. Colin and B. Scrosati, "Rechargeable lithium cells," in *Modern Batteries - An Introduction to Electrochemical Power Sources*, Eastbourne, UK, Butterworth Heinemann, 2003, pp. 198-240.
- [7] M. Daowd, N. Omar, B. Verbrugge, P. Van Den Bossche, and J. Van Mierlo, Battery Models Parameter Estimation based on Matlab/Simulink, World Battery, Hybrid and Fuel Cell Electric Vehicle Symposium & Exhibition, Shenzhen, China, Nov. 5, 2010, pp. 1-6.
- [8] Ran, Z.Y., Wang, J.P., Chen, Y.H., Wang, Y., Si, X.Y.: Battery Management System Used for HEV. *Journal of Chongqing University of Technology* 24(2), 2010, pp. 1–5
- [9] T. R. Jow, S. A. Delp, J. L. Allen, J.-P. Jones, and M. C. Smart, "Factors limiting lithium/supercapacitor transfer kinetics in li-ion batteries," *Journal of The Electrochemical Society*, vol. 165, no. 2, pp. A361–A367, 2018.
- [10] G. J. Plett, "Colorado springs," *Journal of The Electrochemical Society*.
- [11] J. Edge, S. O’Kane, R. Prosser, N. Kirkaldy, A. Patel, A. Hales, A. Ghosh, W. Ai, J. Chen, J. Jiang, S. Li, M.-C. Pang, L. Bravo Diaz, A. Tomaszewska, M. Marzook, K. Radhakrishnan, H. Wang, Y. Patel, B. Wu, and G. Offer, "Lithium ion battery degradation: What you need to know," *Physical Chemistry Chemical Physics*, vol. 23, 04 2021.
- [12] M. Doyle and J. Newman, "The use of mathematical modeling in the design of lithium/polymer battery systems," *Electrochimica Acta*, vol. 40, no. 13, pp. 2191–2196, 1995. International symposium on polymer electrolytes.
- [13] M. Doyle and J. Newman, "The use of mathematical modeling in the design of lithium/polymer battery systems," *Electrochimica Acta*, vol. 40, no. 13, pp. 2191–2196, 1995. International symposium on polymer electrolytes.
- [14] M. Doyle, T. F. Fuller, and J. Newman, "Modeling of galvanostatic charge and discharge of the lithium/polymer/insertion cell," *Journal of The Electrochemical Society*, vol. 140, pp. 1526–1533, Jun 1993.
- [15] T. F. Fuller, M. Doyle, and J. Newman, "Simulation and optimization of the dual lithium ion insertion cell," *Journal of The Electrochemical Society*, vol. 141, pp. 1–10, Jan 1994.
- [16] C. M. Doyle, "Design and Simulation of Lithium Rechargeable Batteries," Ph.D. Thesis, 1995
- [17] G. L. Plett and M. S. Trimboli, *Battery management systems. Volume 3: Physics-based methods /*

- Gregory L. Plett, M. Scott Trimboli. in Artech House power engineering library. Boston London: Artech House, 2024.
- [18] H. He, R. Xiong, and J. Fan, "Evaluation of Lithium-Ion Battery Equivalent Circuit Models for State of Charge Estimation by an Experimental Approach," *Energies*, vol. 4, no. 4, pp. 582–598, Mar. 2011, doi: 10.3390/en4040582.
- [19] M.-K. Tran et al., "A comprehensive equivalent circuit model for lithium-ion batteries, incorporating the effects of state of health, state of charge, and temperature on model parameters," *Journal of Energy Storage*, vol. 43, p. 103252, Nov. 2021, doi: 10.1016/j.est.2021.103252.
- [20] L. Zhang, H. Peng, Z. Ning, Z. Mu, and C. Sun, "Comparative Research on RC Equivalent Circuit Models for Lithium-Ion Batteries of Electric Vehicles," *Applied Sciences*, vol. 7, no. 10, p. 1002, Sep. 2017, doi: 10.3390/app7101002.
- [21] X. Hua, C. Zhang, and G. Offer, "Finding a better fit for lithium ion batteries: A simple, novel, load dependent, modified equivalent circuit model and parameterization method," *Journal of Power Sources*, vol. 484, p. 229117, Feb. 2021, doi: 10.1016/j.jpowsour.2020.229117.
- [22] N. Meddings et al., "Application of electrochemical impedance spectroscopy to commercial Li-ion cells: A review," *Journal of Power Sources*, vol. 480, p. 228742, Dec. 2020, doi: 10.1016/j.jpowsour.2020.228742.
- [23] T. Stanciu, D.-I. Stroe, R. Teodorescu, and M. Swierczynski, "Extensive EIS characterization of commercially available lithium polymer battery cell for performance modelling," in 2015 17th European Conference on Power Electronics and Applications (EPE'15 ECCE-Europe), Geneva: IEEE, Sep. 2015, pp. 1–10. doi: 10.1109/EPE.2015.7309443.
- [24] H. Nunes, J. Martinho, J. Fermeiro, J. Pombo, S. Mariano, and M. D. R. Calado, "Impedance analysis of a lithium-ion battery using the electrochemical impedance spectroscopy," in 2022 IEEE International Conference on Environment and Electrical Engineering and 2022 IEEE Industrial and Commercial Power Systems Europe (EEEIC / I&CPS Europe), Prague, Czech Republic: IEEE, Jun. 2022, pp. 1–7. doi: 10.1109/EEEIC/ICPSEurope54979.2022.9854629.
- [25] Q.-A. Huang, Y. Shen, Y. Huang, L. Zhang, and J. Zhang, "Impedance Characteristics and Diagnoses of Automotive Lithium-Ion Batteries at 7.5% to 93.0% State of Charge," *Electrochimica Acta*, vol. 219, pp. 751–765, Nov. 2016, doi: 10.1016/j.electacta.2016.09.154.
- [26] Z. Ren and C. Du, "A review of machine learning state-of-charge and state-of-health estimation algorithms for lithium-ion batteries," *Energy Reports*, vol. 9, pp. 2993–3021, Dec. 2023, doi: 10.1016/j.egyr.2023.01.108.
- [27] B. Balasingam, *Robust battery management system design with Matlab*. in Artech House Power Engineering. Boston London: Artech House, 2023.
- [28] S. Li, H. He, J. Li, and H. Wang, Big Data Driven Deep Learning algorithm based lithium-ion battery SOC estimation method: A hybrid mode of C-BMS and V-BMS, Feb. 2020. doi:10.46855/energy-proceedings-555
- [29] Kollmeyer, P., 2018. Panasonic 18650PF li-ion battery data. In: Mendeley Data, Vol. 1. <http://dx.doi.org/10.17632/WYKHT8Y7TG.1>.
- [30] Naguib, M., Kollmeyer, P., Skells, M., 2020. LG 18650hg2 li-ion battery data and example deep neural network xEV SOC estimator script. In: Mendeley Data, V3. Mendeley Data, <http://dx.doi.org/10.17632/CP3473X7XV.3>.
- [31] Severson, K.A., et al., 2019. Data-driven prediction of battery cycle life before capacity degradation. *Nat. Energy* 4 (5), 383–391. <http://dx.doi.org/10.1038/s41560-019-0356-8>.
- [32] University of Maryland, 2021. Battery data | center for advanced life cycle engineering (CALCE). In:

Battery Data. <https://calce.umd.edu/battery-data> (accessed Sep. 21, 2021).

- [33] Barkholtz, H.M., Fresquez, A., Chalamala, B.R., Ferreira, S.R., 2017. A database for comparative electrochemical performance of commercial 18650-format lithium-ion cells. J. Electrochem. Soc. 164 (12), A2697–A2706. <http://dx.doi.org/10.1149/2.1701712jes>.
- [34] Saha, K., Goebel, B., 2007. Battery Data Set. NASA Ames Prognostics Data Repository, NASA Ames, Moffett Field, CA, [[http://ti.arc.nasa.gov/project/prognostic data-repository](http://ti.arc.nasa.gov/project/prognostic-data-repository)]
- [35] Christoph, R.B., 2017. Diagnosis and Prognosis of Degradation in Lithium-Ion Batteries (Ph. D. Thesis). Department of Engineering Science, University of Oxford.
- [36] E. Kurt, “PHYSICS BASED MODELING OF LITHIUM-ION BATTERIES FOR ELECTRIFIED VEHICLE SIMULATIONS,” Sabanci University, 2022.
- [37] P. Khumprom and N. Yodo, “A data-driven predictive prognostic model for lithium-ion batteries based on a deep learning algorithm,” Energies, vol. 12, no. 4, 2019.
- [38] C. Wang, N. Lu, S. Wang, Y. Cheng, and B. Jiang, “Dynamic long short-term memory neural-network- based indirect remaining-useful-life prognosis for satellite Lithium-ion battery,” Appl. Sci., vol. 8, no. 11, 2018.
- [39] Parte del código utilizado está basado en: <https://github.com/Kalrfou/CapstoneProject>

备注	
----	--